

# Class-E<sup>2</sup> Capacitive Wireless Power Transfer DC-DC Converter for LED Lighting Applications

L. Solimene\*, F. Corti\*\*, S. Musumeci\*, A. Reatti\*\*, C. S. Ragusa\*,

\* Department of Energy, Politecnico di Torino, Torino, (Italy)

\*\*DINFO, University of Florence, Florence, (Italy)

**Abstract**—In this paper, a Capacitive Wireless Power Transfer (CWPT) Class-E2 DC-DC converter for LED lighting application is presented. The design procedure to operate under Zero Voltage Switching (ZVS) conditions is proposed. The design procedure of the rectifier and the impedance matching with the CWPT is analyzed. The achievement of ZVS condition and the desired output power under the nominal operating condition are evaluated with several simulation results.

**Index Terms**— LED Lighting, Class-E inverter, DC-DC Power Converter.

## I. INTRODUCTION

LEDs (Light Emitting Diodes) offer several advantages over traditional lighting sources. Firstly, this technology can produce the same amount of light as traditional lighting sources while using significantly less power [1]. In addition, LEDs have a much longer lifespan than traditional lighting sources leading to significant cost savings over time [2]. Finally, they are environmentally friendly and are characterized by higher resistance to shock and vibration, making them ideal for use in harsh environments and increasing durability [3].

LED lighting requires a constant and stable power source to operate efficiently and effectively. DC-DC power converters can provide this by converting the voltage of the power source to a level that is suitable for LED lights [4]. This ensures that the LEDs receive the right amount of power they need while minimizing energy waste and increasing lifespan [5]. Additionally, a DC-DC power converter allows LED lights to be used with a wider range of power sources, including batteries and solar panels [6]. This is important for applications with limited or unavailable access to an AC power source [7].

One of the primary characteristics required of a LED driver is its conversion efficiency [8]-[9]. If the driver converter is not well designed, a large amount of power will be dissipated, which may overheat the LED lamp, reducing its lifespan [10]. Another important aspect is related to Electromagnetic Interference (EMI) [11]. In fact, LED drivers can generate electrical noise that can interfere with other electronic devices or cause flickering in the LED lighting [12].

These two main problems could be solved using resonant converters. Soft switching techniques minimize switching losses by ensuring that the voltage or current waveforms transition smoothly between their high and low states, reducing the amount of energy lost as heat during each switching cycle [13]. This is typically achieved by carefully tuning the resonant circuit, allowing for a smooth and efficient transfer of energy between the input and output of the converter [14]-[15]. This allows for operating at a higher switching frequency, leading to the miniaturization process of the LED driver, which usually cannot be excessively bulky.

Since the overall dimensions must be minimized, choosing the topology is a key aspect. The Class-E resonant converter is an excellent compromise between conversion efficiency and overall dimensions. In fact, this converter is characterized by a single power switch. Still, thanks to the ability to work in Zero Voltage Switching (ZVS) conditions, it can manage power ratings compatible with LED lighting applications using a minimum number of components. Additionally, if properly sized, this topology can achieve Zero Derivative Switching (ZDS), minimizing EMI issues [16]-[18].

This topology has already been widely used for LED lighting applications [19]-[25].

In this paper, a Class-E converter is used to supply a LED lamp exploiting Capacitive Wireless Power Transfer (CWPT). Differently from Inductive Wireless Power Transfer (IWPT), this technology uses electric fields to transmit electrical power wirelessly between a transmitter and a receiver. Usually, the transmitter and the receiver consist of aluminum plates separated by a small distance. The transmitter generates a high-frequency AC voltage that is applied across the transmitting electrodes, creating an electric field that extends into the space between the electrodes [26]. When the receiver is placed within this electric field, an electrical current is induced in the receiving electrodes.

The paper is organized as follows. In Section II, the simplified model of the CWPT system is presented. In Section III, the equivalent electrical model of LED lighting is explored. In Section IV, the design procedures of the Class-E inverter and Class-E rectifier are presented. The

circuit is simulated in PLECS, and the results are shown in Section V. Finally, in Section VI, the obtained results are discussed.

## II. CAPACITIVE WIRELESS POWER TRANSFER MODELING

In Fig. 1, the capacitive four plates systems are shown. The plates  $P_1$  and  $P_2$  are located on the primary side, while plates  $P_3$  and  $P_4$  are on the secondary side. The capacitances  $C_{ij}$  model the electric coupling between the plate  $P_i$  and  $P_j$ .

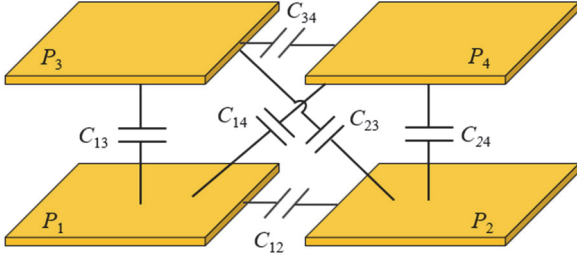


Fig. 1. Four plates capacitive system and related capacitances.

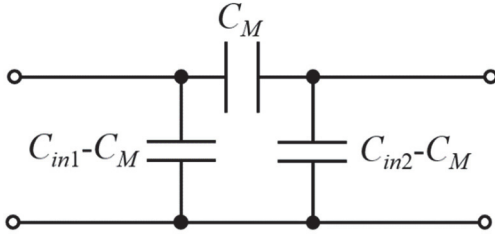


Fig. 2. Equivalent electrical model of CWPT system.

Several equivalent electric circuits have been proposed in the literature. In this paper, the  $\pi$ -equivalent model, proposed in [27], is adopted. The four plates can be equivalently represented by three capacitors, as shown in Fig. 2. The values of each capacitance can be calculated as

$$C_M = \frac{C_{24}C_{13} - C_{14}C_{23}}{C_{13} + C_{14} + C_{23} + C_{24}} \quad (1)$$

$$C_{in1} = C_{12} + \frac{(C_{13} + C_{14})(C_{23} + C_{24})}{C_{13} + C_{14} + C_{23} + C_{24}} \quad (2)$$

$$C_{in2} = C_{34} + \frac{(C_{13} + C_{23})(C_{14} + C_{24})}{C_{13} + C_{14} + C_{23} + C_{24}} \quad (3)$$

It is assumed that the distance between  $P_1$ - $P_3$  and  $P_2$ - $P_4$  is large enough to neglect the cross-couplings  $C_{12}$ ,  $C_{14}$ ,  $C_{23}$ , and  $C_{34}$ . In addition, it is assumed that the plates have the same dimension. Under these assumptions, the capacitive coupling can be simply modelled with a capacitance  $C_M = C/2$ .

The capacitance between two square plates must also consider the fringing field effects, which are more significant when the distance between  $P_1$ - $P_3$  and  $P_2$ - $P_4$  is comparable with the plate dimension. Several studies have been performed to estimate the coupling between square metal plates [28]-[29]. In [29], the coupling between two square plates with side  $l$  separated by an airgap  $d$  is

$$C = \varepsilon_0 \varepsilon_r \left[ 1 + 2.34 \left( \frac{d}{w} \right)^{0.891} \right] \left( \frac{l^2}{d} \right) \quad (4)$$

Where  $w$  is the width of the plates and  $\varepsilon = \varepsilon_0 \varepsilon_r = 8.875 \cdot 10^{-12}$  F/m is the dielectric constant of air.

Assuming the use plates with  $l = 50$  mm,  $w = 2$  mm, and operating with an air gap  $d = 10$  mm, a capacitance  $C_M = 2.31$  nF is obtained. Thus, neglecting the cross-coupling capacitances, the electrical coupling between the four plates can be modeled by an equivalent capacitance  $C = C_M / 2 = 1.16$  nF.

## III. LED LIGHTNING MODELING

The electrical equivalent model of a light-emitting diode (LED) is typically represented using a combination of a diode and a current source. The diode represents the non-linear current-voltage (I-V) characteristics of the LED, while the current source represents the light emission of the LED, which is proportional to the current flowing through it.

The I-V characteristics of an LED are non-linear and can be described using an exponential function. The forward voltage drops across the LED, which is typically around 2 to 3 volts, depending on the LED material and colour and on the current through the LED. At low voltages, the LED has a high resistance and a low current flow. Once the forward voltage reaches the threshold value, the LED turns on, and the current through the LED increases rapidly with a small increase in voltage as follows:

$$i = I_S \left( e^{\frac{qV}{NkT_m}} - 1 \right) \quad (5)$$

where  $q$  is the elementary charge on an electron,  $k$  is the Boltzmann constant,  $N$  is the emission coefficient,  $I_S$  is the saturation current, and  $T_m$  is the temperature at which the diode parameters are specified.

In Table I, the characteristics of the LED used in this paper are summarized.

TABLE I. LED CHARACTERISTICS

| Parameter | Description                      | Value                          |
|-----------|----------------------------------|--------------------------------|
| $q$       | Elementary Charge on an Electron | $1.602176 \cdot 10^{-19}$ C    |
| $k$       | Boltzmann Constant               | $1.3806503 \cdot 10^{-23}$ J/K |
| $N$       | Emission Coefficient             | 10                             |
| $I_s$     | Saturation Current               | $5 \cdot 10^{-7}$ A            |
| $T_m$     | Measurement Temperature          | 25°C                           |

In the electrical equivalent model, the diode is typically represented using a current-controlled current source, where the current source produces a current that is proportional to the exponential function of the diode voltage.

## IV. CLASS-E DC-DC CONVERTER DESIGN

Once the capacitive coupling  $C_M$  has been estimated and the LED load modeled, the design of the Class-E inverter

and rectifier that allows to delivery of the desired output power operating in ZVS condition is presented. The electrical constraints of the proposed circuits are summarized in Table II.

TABLE II. LED CHARACTERISTICS

| Parameter | Description         | Value       |
|-----------|---------------------|-------------|
| $f_s$     | Operating Frequency | 2 MHz       |
| $R_L$     | Load Resistance     | 10 $\Omega$ |
| $I_o$     | Output Current      | 2.2 A       |

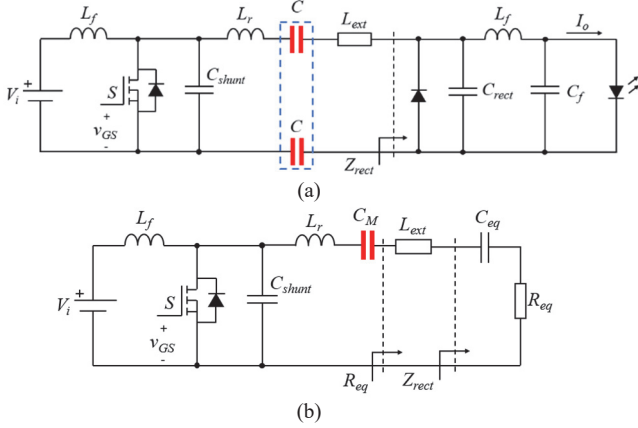


Fig. 3. Class-E2 resonant converter. (a) Electrical circuit. (b) Circuit with the equivalent model of the rectifier.

where  $\omega$  is the angular frequency, and  $R_{eq}$  is the equivalent resistance seen by the inverter, as shown in Fig. 3(a). Since the impedance of the rectifier  $Z_{rect}$  has a real and imaginary part, an external inductance is added, such as  $X_{ext} = -X_{rect}$ . In this way, the impedance  $R_{eq}$  seen by the inverter is purely resistive, and ZVS can be reached.

#### A. Class-E Low $dv/dt$ Rectifier with Parallel Capacitor

A Class E low  $dv/dt$  rectifier with a parallel capacitor is shown in Fig. 3(a). The rectifier consists of a diode, a shunt capacitor  $C$ , and a second-order low-pass output filter  $L_f$ - $C_f$ . As shown in [30], the equivalent resistance can be calculated by the following equations:

$$\tan(\varphi) = \frac{1 - \cos(2\pi D)}{2\pi(1-D) + \sin(2\pi D)} \quad (6)$$

$$\frac{R_{eq}}{R_L} = 2 \sin^2(\varphi) \quad (7)$$

$$\omega C_{rect} R_{eq} = \omega C_{rect} R_L \frac{R_{eq}}{R_L} = \frac{\sin^2 \varphi}{\pi} \left[ 1 - 2\pi^2(1-D)^2 - \cos(2\pi D) + \frac{2\pi(1-D) + \sin(2\pi D)}{\tan \varphi} \right] \quad (8)$$

#### B. Class-E DC-AC Inverter

The topology of the Class-E inverter is shown in Fig. 3(b). In this paper, the design procedure presented in [30] has been used to design the components. Assuming to operate

at a constant duty cycle  $D$ , the components can be designed using the equations:

$$\frac{C_{eq}}{C} = \pi \left[ \pi(1-D) + \sin(2\pi D) - \frac{1}{4} \cos(2\varphi) \sin(4\pi D) - \frac{1}{2} \sin(2\varphi) \sin^2(2\pi D) - 2\pi(1-D) \sin \varphi \sin(2\pi D - \varphi) \right]^{-1} \quad (9)$$

Assuming to operate at fixed duty cycle  $D=0.5$ , the previous equations can be simplified to  $C_{rect}=1/(\pi\omega R_L)$ ,  $R_{eq}=0.5768 \cdot R_L$  and  $C_{eq}=4.726 \cdot C_{rect}$ . The transformer turn ratio  $n$  is assumed to be  $n=1$ . Using the previous equations and assuming to operate at a constant frequency  $f_s=2\text{MHz}$  and duty cycle  $D=0.5$ , the components' values are summarized in Table III.

A load resistor  $R_L=10 \Omega$  was selected to obtain an output voltage and current compatible with this application.

TABLE III. LED CHARACTERISTICS

| Parameter | Description                 | Value              |
|-----------|-----------------------------|--------------------|
| $R_L$     | Load Resistance             | 10 $\Omega$        |
| $C_f$     | Filter Capacitance          | 10 $\mu\text{F}$   |
| $L_f$     | Filter Inductance           | 100 $\mu\text{H}$  |
| $C_{eq}$  | Equivalent Capacitance      | 12 nF              |
| $L_{ext}$ | External Inductance         | 0.52 $\mu\text{H}$ |
| $V_F$     | Diode Forward Voltage       | 0.3 V              |
| $r_F$     | Diode Conduction Resistance | 0.1 $\Omega$       |

$$V_i = \sqrt{\frac{\pi^2 + 4}{8}} P_o R_{eq} \quad (10)$$

$$C_{shunt} = \frac{8}{\pi(\pi^2 + 4)} \frac{1}{\omega C_1 R_{eq}} \quad (11)$$

$$L_r = \frac{Q_L R_{eq}}{\omega} \quad (12)$$

$$C_r = \frac{1}{\omega R_{eq} \left( Q_L - \frac{\pi(\pi^2 - 4)}{16} \right)} \quad (13)$$

$$L_f = \frac{14\pi R_{eq}}{\omega} \quad (14)$$

Where  $Q_L$  is the quality factor and  $R_{eq}$  is the equivalent resistance of the rectifier. Using the values shown in Table II, the values of the components using (6)-(10) are summarized in Table IV.

## V. SIMULATION RESULTS

A PLECS simulation has been performed, as shown in Fig.4

TABLE IV. LED CHARACTERISTICS

| Parameter                | Description                              | Value                       |
|--------------------------|--|-----------------------------|
| $L_f / r_{Lf}$           | Choke Inductor / Parasitic Resistance    | 200 $\mu$ H / 50 m $\Omega$ |
| $C_{shunt} / r_{Cshunt}$ | Shunt Capacitor / Parasitic Resistance   | 1.9 nF / 50 m $\Omega$      |
| $V_i$                    | Input DC Voltage                         | 25.8 V                      |
| $L_r / r_{Lr}$           | Resonant Inductor / Parasitic Resistance | 6.1 $\mu$ H / 50 m $\Omega$ |

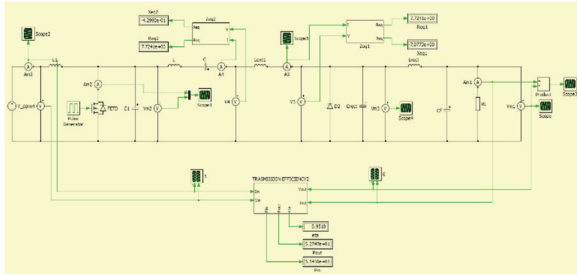


Fig. 4. PLECS simulation schematic of the electrical circuit.

In Fig. 5, the drain-to-source voltage and current waveforms on the MOSFET are shown. As it can be seen the ZVS condition is reached, leading to low switching losses.

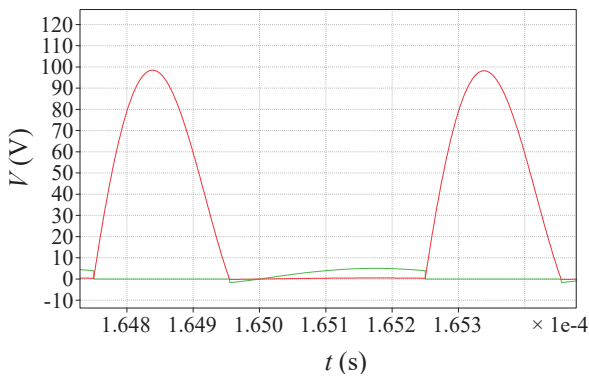


Fig. 5. Power MOSFET drain-to-source voltage (red trace) and drain-to-source current (green trace).

In Fig. 6 the current on the resonant tank is shown. As expected, since the converter operates in resonance, the current is approximately sinusoidal.

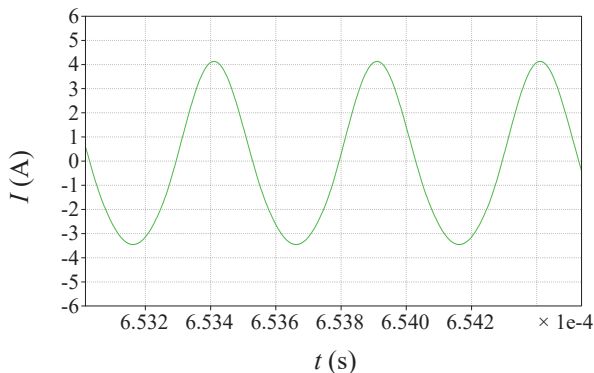


Fig. 6. Primary resonant current.

In Fig. 7, the voltage and the current on the rectifier diode is shown. As it can be seen, also here the ZVS condition is reached, leading to low power losses.

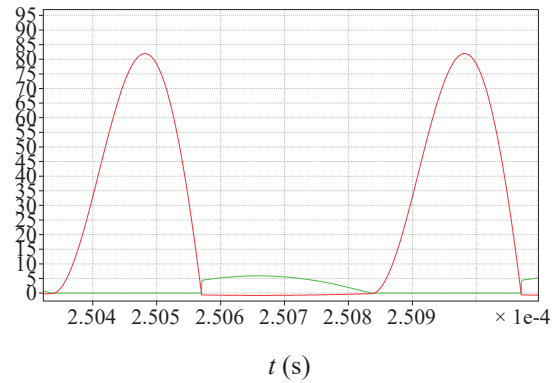


Fig. 7. Voltage across the rectifier diode (red trace) and current (green trace).

Finally, in Fig. 8, the transient of the output power is shown. As it can be seen, the desired value of output power is reached, allowing to light the LEDs.

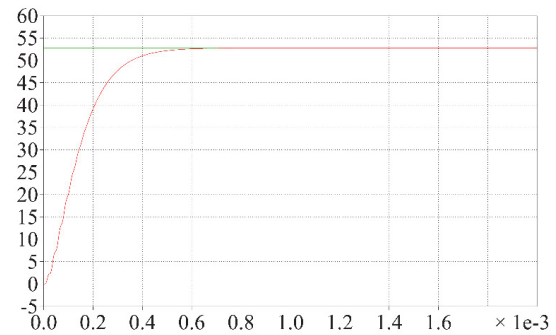


Fig. 8. Transient of the output voltage  $v_o$  (red trace) and target value (green trace).

The DC-DC conversion efficiency measured by simulation is  $\eta_{DC-DC} = 0.96$ .

## VI. CONCLUSIONS

In this paper a Class-E<sup>2</sup> CWPT DC-DC converter for lighting applications is presented. The model of the electric coupling between capacitive plates is presented. Starting from the model of the LEDs load, the design procedure of the Class-E rectifier is proposed. The impedance matching required to obtain operate the Class-E inverter at ZVS is presented. The performance of the CWPT system is evaluated through several PLECS simulation.

## REFERENCES

- [1] R. -L. Lin, J. -Y. Tsai, S. -Y. Liu and H. -W. Chiang, "Optimal Design of LED Array Combinations for CCM Single-Loop Control LED Drivers," in *IEEE Journal of Emerging and Selected Topics in Power Electronics*, vol. 3, no. 3, pp. 609-616, Sept. 2015.
- [2] D. Park, Z. Liu and H. Lee, "A 40 V 10 W 93%-Efficiency Current-Accuracy-Enhanced Dimmable LED Driver With Adaptive Timing Difference Compensation for Solid-State Lighting Applications," in *IEEE Journal of Solid-State Circuits*, vol. 49, no. 8, pp. 1848-1860, Aug. 2014.
- [3] M. Martins, M. S. Perdigão, A. M. S. Mendes, R. A. Pinto and J. M. Alonso, "Analysis, Design, and Experimentation of a Dimmable Resonant-Switched-Capacitor LED Driver With Variable Inductor Control," in *IEEE Transactions on*

- Power Electronics*, vol. 32, no. 4, pp. 3051-3062, April 2017, doi: 10.1109/TPEL.2016.2575918.
- [4] K. Zhou, J. G. Zhang, S. Yuvarajan and D. F. Weng, "Quasi-Active Power Factor Correction Circuit for HB LED Driver," in *IEEE Transactions on Power Electronics*, vol. 23, no. 3, pp. 1410-1415, May 2008.
  - [5] S. Musumeci, C. S. Ragusa, M. Palma and L. Solimene, "Low-Voltage GaN FET in High Power Density Half-Bridge LED Driver," 2021 AEIT International Annual Conference (AEIT), Milan, Italy, 2021, pp. 1-6, doi: 10.23919/AEIT53387.2021.9626936.
  - [6] V. Barba, L. Solimene, M. Palma, S. Musumeci, C. S. Ragusa and R. Bojoi, "Modelling and Experimental Validation of GaN Based Power Converter for LED Driver," 2022 IEEE International Conference on Environment and Electrical Engineering and 2022 IEEE Industrial and Commercial Power Systems Europe (EEEIC / I&CPS Europe), Prague, Czech Republic, 2022, pp. 1-6, doi: 10.1109/EEEIC/ICPSEurope54979.2022.9854660.
  - [7] A. Barad, S. Tungar, N. Sangle, K. Bharambe and D. P. Kadam, "Solar panel based multi-mobile charger with LED illumination," 2017 *International Conference on Innovations in Information, Embedded and Communication Systems (ICIIECS)*, Coimbatore, India, 2017, pp. 1-4.
  - [8] K. T. Thanh, H. Yahoui, N. Siauve, N. -O. Nam and D. Genon-Catalot, "Construct and control a PV-based independent public LED street lighting system with an efficient battery management system based on the power line communication," 2017 *IEEE Second International Conference on DC Microgrids (ICDCM)*, Nuremberg, Germany, 2017, pp. 497-501.
  - [9] S. Jang and M. W. Shin, "Thermal Analysis of LED Arrays for Automotive Headlamp With a Novel Cooling System," in *IEEE Transactions on Device and Materials Reliability*, vol. 8, no. 3, pp. 561-564, Sept. 2008, doi: 10.1109/TDMR.2008.2002355.
  - [10] S. Musumeci, "Passive and Active Topologies Investigation for LED Driver Circuits", in *Light-Emitting Diodes and Photodetectors - Advances and Future Directions*. London, United Kingdom: IntechOpen, 2021 [Online]. Available: <https://www.intechopen.com/chapters/76115> doi: 10.5772/intechopen.97098
  - [11] Y. Deshaves, R. Baillot, S. Joly, Y. Ousten and L. Béchou, "Overview on Sustainability, Robustness, and Reliability of GaN Single-Chip LED Devices," in *IEEE Transactions on Device and Materials Reliability*, vol. 15, no. 4, pp. 621-625, Dec. 2015, doi: 10.1109/TDMR.2015.2488978.
  - [12] L. Svilainis, "Comparison of the EMI Performance of LED PWM Dimming Techniques for LED Video Display Application," in *Journal of Display Technology*, vol. 8, no. 3, pp. 162-165, March 2012.
  - [13] Pugi Luca, Alberto Reatti, Fabio Corti, "Application of Wireless Power Transfer to Railway Parking Functionality: Preliminary Design Considerations with Series-Series and LCC Topologies", *Journal of Advanced Transportation*, Volume 2018, Article number 8103140, DOI 10.1155/2018/8103140.
  - [14] P. Luca, A. Reatti, F. Corti and R. A. Mastromauro, "Inductive power transfer: Through a bondgraph analogy, an innovative modal approach," 2017 IEEE International Conference on Environment and Electrical Engineering and 2017 IEEE Industrial and Commercial Power Systems Europe (EEEIC / I&CPS Europe), Milan, Italy, 2017, pp. 1-6, doi: 10.1109/EEEIC.2017.7977737.
  - [15] M. Pierini et al., "Application of induction power recharge to garbage collection service," 2017 IEEE 3rd International Forum on Research and Technologies for Society and Industry (RTSI), Modena, Italy, 2017, pp. 1-5, doi: 10.1109/RTSI.2017.8065961.
  - [16] Corti F, Reatti A, Wu Y-H, Czarkowski D, Musumeci S. Zero Voltage Switching Condition in Class-E Inverter for Capacitive Wireless Power Transfer Applications. *Energies*. 2021; 14(4):911. <https://doi.org/10.3390/en14040911>.
  - [17] A. Reatti, S. Musumeci and F. Corti, "Class-E Inverters for Capacitive Wireless Power Transfer in Charger Circuit Applications," 2021 AEIT International Conference on Electrical and Electronic Technologies for Automotive (AEIT AUTOMOTIVE), Torino, Italy, 2021, pp. 1-5, doi: 10.23919/AEITAUTOMOTIVE52815.2021.9662732.
  - [18] L. Solimene, F. Corti, S. Musumeci, A. Reatti and C. Ragusa, "Extended ZVS/ZCS operation of Class-E Inverter for Capacitive Wireless Power Transfer," 2022 IEEE International Conference on Environment and Electrical Engineering and 2022 IEEE Industrial and Commercial Power Systems Europe (EEEIC / I&CPS Europe), Prague, Czech Republic, 2022, pp. 1-6, doi: 10.1109/EEEIC/ICPSEurope54979.2022.9854655.
  - [19] J. Ribas, P. J. Quintana-Barcia, J. Cardesin, A. J. Calleja and E. L. Corominas, "LED Series Current Regulator Based on a Modified Class-E Resonant Inverter," in *IEEE Transactions on Industrial Electronics*, vol. 65, no. 12, pp. 9488-9497, Dec. 2018, doi: 10.1109/TIE.2018.2822618.
  - [20] Y. Wang, J. Huang, W. Wang and D. Xu, "A Single-Stage Single-Switch LED Driver Based on Class-E Converter," in *IEEE Transactions on Industry Applications*, vol. 52, no. 3, pp. 2618-2626, May-June 2016.
  - [21] Ö. Ö. Zengin, M. Boztepe and A. Tekin, "Class E Resonant Converter Design for LED Drivers," 2019 *1st Global Power, Energy and Communication Conference*, Nevsehir, Turkey, 2019, pp. 128-133.
  - [22] T. Sangsuwan, C. Ekkaravarodome, S. Mangkalaiarn, S. Sukanna, K. Jirasereamongkul and K. Higuchi, "A Single-Stage High-Power-Factor LED Driver based on Interleaved ZCDS Class-E Rectifier," 2019 *Research, Invention, and Innovation Congress (RI2C)*, Bangkok, Thailand, 2019, pp. 1-4, doi: 10.1109/RI2C48728.2019.8999917.
  - [23] I. Saisuksaard and P. Chansri, "An Electroluminescent driven with Class E Resonant Inverter," 2022 *International Electrical Engineering Congress (iEECON)*, Khon Kaen, Thailand, 2022, pp. 1-4.
  - [24] S. Mangkaliaian, C. Ekkaravarodome, K. Jirasereamongkul, P. Thonthong, K. Higuchi and M. K. Kazimierzczuk, "A Single-Stage LED Driver Based on ZCDS Class-E Current-Driven Rectifier as a PFC for Street-Lighting Applications," in *IEEE Transactions on Power Electronics*, vol. 33, no. 10, pp. 8710-8727, Oct. 2018, doi: 10.1109/TPEL.2017.2780088.
  - [25] Y. Wang, J. Huang, G. Shi, W. Wang and D. Xu, "A Single-Stage Single-Switch LED Driver Based on the Integrated SEPIC Circuit and Class-E Converter," in *IEEE Transactions on Power Electronics*, vol. 31, no. 8, pp. 5814-5824, Aug. 2016, doi: 10.1109/TPEL.2015.2489464.
  - [26] A. Reatti, L. Pugi, F. Corti and F. Grasso, "Effect of Misalignment in a Four Plates Capacitive Wireless Power Transfer System," 2020 IEEE International Conference on Environment and Electrical Engineering and 2020 IEEE Industrial and Commercial Power Systems Europe (EEEIC / I&CPS Europe), Madrid, Spain, 2020, pp. 1-4, doi: 10.1109/EEEIC/ICPSEurope49358.2020.9160627.
  - [27] Lecluyse C, Minnaert B, Kleemann M. A Review of the Current State of Technology of Capacitive Wireless Power Transfer. *Energies*. 2021; 14(18):5862. <https://doi.org/10.3390/en14185862>
  - [28] D. Vincent, P. A. V. J. S. and S. S. Williamson, "Feasibility Analysis of a Reduced Capacitive Wireless Power Transfer System Model for Transportation Electrification Applications," in *IEEE Journal of Emerging and Selected Topics in Industrial Electronics*, vol. 3, no. 3, pp. 474-481, July 2022, doi: 10.1109/JESTIE.2021.3116523.
  - [29] H. Nishiyama and M. Nakamura, "Form and capacitance of parallel-plate capacitors," in *IEEE Transactions on Components, Packaging, and Manufacturing Technology: Part A*, vol. 17, no. 3, pp. 477-484, Sept. 1994, doi: 10.1109/95.311759.
  - [30] Marian K. Kazimierzczuk, Dariusz Czarkowski, "Resonant Power Converters, 2nd Edition, Wiley, ISBN: 978-0-470-90538-8, April 2011.